Letter | Editors' Suggestion

Phonon thermal Hall effect in nonmagnetic $Y_2Ti_2O_7$

Rohit Sharma [1,*] Martin Valldor [1,2] and Thomas Lorenz [1,†]

[1] *II. Physikalisches Institut, Universität zu Köln, Zülpicher Strasse 77, 50937 Köln, Germany*

[2] *Centre for Materials Science and Nanotechnology (SMN), Department of Chemistry, University of Oslo, Oslo N-0371, Norway*

(Received 17 July 2024; revised 14 August 2024; accepted 15 August 2024; published 3 September 2024)

We report an investigation of the phonon thermal Hall effect in single crystal samples of $Y_2Ti_2O_7$, $Dy_2Ti_2O_7$, and $DyYTi_2O_7$. We measured the field-linear thermal Hall effect in all three samples. The temperature dependence of thermal Hall conductivities shows a peak around 15 K, which coincides with the peak positions of the longitudinal thermal conductivities. The temperature-dependent longitudinal thermal conductivities indicates that phonons dominate thermal transport in all three samples. However, the presence of Dy^{3+} magnetic ions introduces significant effects on the field dependence of the longitudinal thermal conductivities. The thermal Hall ratio is sizable in all three samples and consistent with the values reported for other insulating materials exhibiting a phononic thermal Hall effect, though their exact underlying mechanism remains yet to be identified. The thermal Hall ratio is nearly the same for $Y_2Ti_2O_7$ and $DyYTi_2O_7$, and slightly larger for $Dy_2Ti_2O_7$, suggesting that magnetic impurities are less significant in generating the phononic thermal Hall effect. Our observations of the phononic thermal Hall effect support an intrinsic origin in $Y_2Ti_2O_7$ and suggest a combination of intrinsic and extrinsic effects in $Dy_2Ti_2O_7$ and $DyYTi_2O_7$.

DOI: 10.1103/PhysRevB.110.L100301

The thermal Hall effect (THE) of phonons observed in various insulating materials continues to be a subject of ongoing debate, particularly regarding its origin and the intrinsic versus extrinsic nature of its underlying mechanisms. Intrinsic mechanisms involve phonon dispersion, including theoretical scenarios such as Berry curvature in phonon bands [1–3], phonon scattering due to collective fluctuations [4,5], and interactions between phonons and other quasiparticles like magnons [6–9]. However, extrinsic mechanisms invoke scattering of phonons by charged impurities or defects [10–16]. Experimentally, phononic THE was first detected in the paramagnetic insulator $Tb_3Ga_5O_{12}$ [17], followed by observations in various other insulating solids [18–41], including nonmagnetic materials [42–45]. The recent observation of phonon THE in several nonmagnetic elemental solids, such as the insulator black phosphorus [43], and semiconductors like Si and Ge [45], has pointed toward the universality of phonon THE in solids. Additionally, the thermal Hall ratio has been phenomenologically shown to exhibit a universal scaling behavior observed across various classes of insulating materials, including nonmagnetic ones [43].

The observation of phonon THE across a wide variety of insulating solids prompted us to reexamine THE in insulating pyrochlore $Y_2Ti_2O_7$, where a previous report by Hirschberger *et al.* [25] indicated a negligible thermal Hall ratio. Another motivation for this revisit is that the study by Hirschberger *et al.* was focused more on the isostructural magnetic material $Tb_2Ti_2O_7$, where a large THE was measured and attributed to exotic neutral excitations associated with its quantum spin liquid state. The thermal Hall ratio measured in $Y_2Ti_2O_7$ was only reported at 15 K, and lead to the conclusion that $Y_2Ti_2O_7$ exhibits null signal, in comparison to the significant THE observed in $Tb_2Ti_2O_7$. Later, Hirokane *et al.* [26] interpreted the observed large THE in $Tb_2Ti_2O_7$ to be of phononic origin, because they measured a comparable thermal Hall signal in a diluted sample in which 70% of the Tb^{3+} ions were replaced by nonmagnetic Y^{3+} ions. This naturally raises the question whether the pure $Y_2Ti_2O_7$ in fact exhibits a null signal or a finite phononic THE, but up to now we are not aware of any systematic study of the THE in $Y_2Ti_2O_7$.

In this letter, we report the discovery of a sizable phonon THE in the nonmagnetic insulator $Y_2Ti_2O_7$ from a comparative study of THE in $Y_2Ti_2O_7$ alongside the isostructural pyrochlore materials $Dy_2Ti_2O_7$ and $DyYTi_2O_7$, which are paramagnetic insulators with large local moments of the Dy^{3+} ions; see Fig. 1. Our discovery of phonon THE in $Y_2Ti_2O_7$ and the related magnetic materials aligns well with observations of the phononic THE measured in various insulating solids [18–21,26,27,32,34,35,40,42–45]. It is noteworthy that $Dy_2Ti_2O_7$ is well-known for spin-ice physics, which involves magnetic monopole excitations resulting from magnetic frustration that prevents the formation of long-range magnetic order [46–49]. The magnetic monopole excitations and their impact on various physical properties (specific heat, thermal conductivity, and magnetization) [50–57], are relevant only at low temperatures ($T < 10$ K) and will not be in the focus of this study.

Single crystals of $Y_2Ti_2O_7$, $Dy_2Ti_2O_7$, and $DyYTi_2O_7$ were grown using the floating-zone technique, starting from sintered bars of TiO_2, Y_2O_3, and Dy_2O_3 mixed in the appropriate stoichiometries. The cool-pressed mixtures were directly introduced in the floating-zone furnace and were

*Contact author: sharma@ph2.uni-koeln.de

†Contact author: tl@ph2.uni-koeln.de

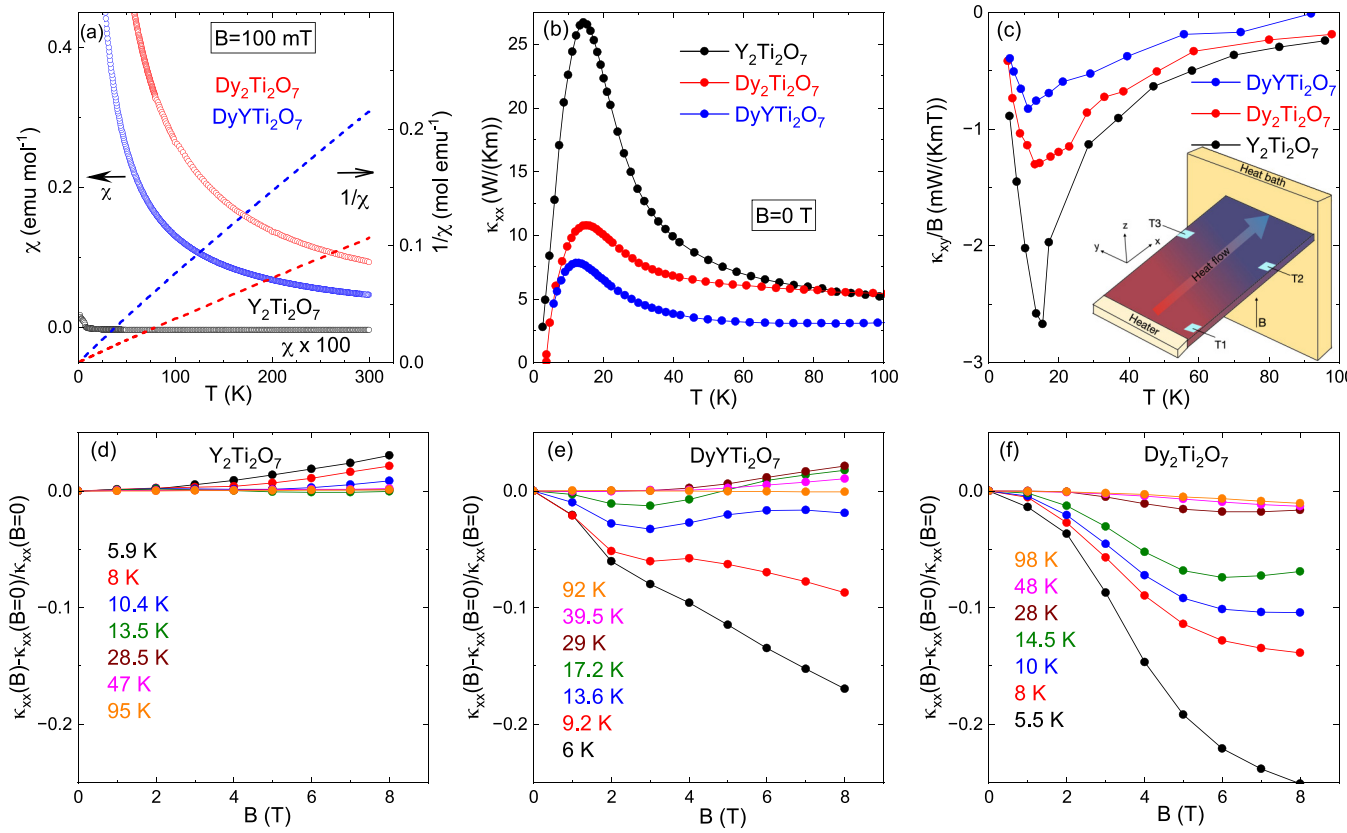

FIG. 1. (a) Magnetic susceptibility of $Dy_2Ti_2O_7$ and $DyYTi_2O_7$ showing Curie-Weiss behavior in comparison to $Y_2Ti_2O_7$, which is nonmagnetic apart from the temperature-independent Core diamagnetism and a tiny impurity contribution (note that χ of $Y_2Ti_2O_7$ is multiplied by 100). (b) Thermal conductivities κ_{xx} of $Y_2Ti_2O_7$, $Dy_2Ti_2O_7$, and $DyYTi_2O_7$ measured in zero magnetic field and (c) the corresponding Thermal Hall conductivities normalized by the field, that is κ_{xy}/B. Panel (c) also displays the schematic setup to measure κ_{xx} and κ_{xy} from the longitudinal and transverse temperature differences ($\Delta T_x = T_1 - T_2$, $\Delta T_y = T_2 - T_3$) induced by a heat current $J_Q \parallel x$ and a magnetic field $B \parallel z$. With respect to the cubic lattice directions, J_Q was along [110] and $B \parallel$ [001] in $Y_2Ti_2O_7$ and $Dy_2Ti_2O_7$, whereas in $DyYTi_2O_7$ the orientations $J_Q \parallel$ [001] and $B \parallel$ [110] were used. (d)–(f) Magnetic field dependencies of κ_{xx} for all three samples, which remains within the range of 3% for $Y_2Ti_2O_7$, but reaches up to 25% for $Dy_2Ti_2O_7$ at the lowest measured temperature.

rapidly run through the melting zone to achieve a prime reaction. Subsequently, the feeding rod and the seed switched places before a slow crystal growth process began, at speeds of typically about 1 mm/h; see also Refs. [52,55]. The thermal conductivities were measured using the standard steady-state, 1-heater 3-thermometer technique under high-vacuum conditions. We employed the steady-state technique where the magnetic field was changed in steps of 1 T from −8 T to 8 T while maintaining the sample temperature at a constant set point. We waited at least 300 s after each incremental change of the magnetic field before taking measurements to avoid transient contaminations caused by magnetocaloric and eddy-current heating effects. The temperature differences, $\Delta T_x = T_1 - T_2$ and $\Delta T_y = T_2 - T_3$, were produced by a 10 kΩ RuO_2 chip resistor (heater) attached at one end of the sample and were measured with magnetic-field calibrated Cernox sensors (CX-1070), as sketched in Fig. 1(c). In the case of $Y_2Ti_2O_7$ and $Dy_2Ti_2O_7$, the heat current $J_Q = RI^2$ was applied along the [110] direction in a perpendicular magnetic field $B \parallel$ [001]. For $DyYTi_2O_7$, the heat current and magnetic field directions were interchanged, i.e., $J_Q \parallel$ [001] and $B \parallel$ [110]. Gold wires were used for making contact on the sample with silver paste and were connected to their respective thermometers of a home-built setup for thermal transport measurements. To eliminate the misalignment of the transverse contacts, the temperature difference ΔT_H was obtained by antisymmetrization of the respective raw data measured in $\pm B$, i.e., $\Delta T_H(B) = (\Delta T_y(T, H) - \Delta T_y(T, -H))/2$. The thermal Hall conductivity is then obtained as $\kappa_{xy} = (\Delta T_H/\Delta T_x)(l/w)\kappa_{xx}$ with longitudinal thermal conductivity $\kappa_{xx} = (J_Q/\Delta T_x)(l/wt)$, distance l between the longitudinal contacts, sample width w, and thickness t.

The temperature dependence of the longitudinal thermal conductivity (κ_{xx}), as shown in Fig. 1(b), measured on $Y_2Ti_2O_7$, $Dy_2Ti_2O_7$, and $DyYTi_2O_7$, exhibits typical phonon behavior with a peak around 15 K. The increase in κ_{xx} at low temperatures, followed by its decrease above the peak temperature, results from the opposite temperature dependencies of phonon heat capacity (C) and phonon mean-free path (l) [58]. Based on kinetic theory, the thermal conductivity $\kappa = \frac{1}{3}Cv\ell$, where C, v, and ℓ represent the phonon-specific heat, sound velocity, and mean-free path, respectively. In insulating solids, the phonon heat conductivity is expected to vary as T^3 in the low-temperature limit, whereas $\frac{1}{T}$ is approached at high temperatures. This arises from the temperature dependencies of C and ℓ, which approach T^3 or

$\frac{1}{T}$ behavior in the respective temperature regimes [59], and $\kappa_{xx}(T)$ is governed by the dominating temperature dependence of either C or ℓ. The absolute values of κ_{xx} for $Y_2Ti_2O_7$ and $Dy_2Ti_2O_7$ are the same at higher temperatures, whereas the peak value for $Y_2Ti_2O_7$ ($\approx$27 W/Km) is significantly larger than for $Dy_2Ti_2O_7$ ($\approx$12 W/Km). The measured $\kappa_{xx}(T)$ for both, $Y_2Ti_2O_7$ and $Dy_2Ti_2O_7$, are in good agreement with those previously reported [18,53,60,61]. The $\kappa_{xx}(T)$ for $DyYTi_2O_7$ remains smaller than the other two across the entire temperature range and shows a peak value of $\approx$8 W/Km. The reduced $\kappa_{xx}(T)$ values in $DyYTi_2O_7$ compared to the pure compounds are likely due to the additional disorder introduced by the statistical distribution of Dy and Y ions. The fact that $Y_2Ti_2O_7$ has a larger thermal conductivity peak than $Dy_2Ti_2O_7$ can be attributed to additional presence of magnetic scattering in the latter, which leads to extra suppression of κ_{xx}. $Y_2Ti_2O_7$ is nonmagnetic, whereas $Dy_2Ti_2O_7$ has a local magnetic moment $\mu \simeq 10\,\mu_B/Dy^{3+}$, in agreement with Hund's rules. Therefore, phonon scattering due to magnetic Dy^{3+} ions could also be a potential source of suppressed κ_{xx} at low temperatures for $Dy_2Ti_2O_7$ and $DyYTi_2O_7$ samples. The strong suppression of κ_{xx} for $DyYTi_2O_7$ is the combined effect of disorder induced by the random distribution of Dy and Y ions, and the magnetic scattering of phonons compared to the parent compound $Dy_2Ti_2O_7$.

Figures 1(d)–1(f) show κ_{xx} as a function of the magnetic field at different temperatures. For $Y_2Ti_2O_7$, the field dependence is negligible at higher temperatures and very weak (below about 3%) at low temperatures. In contrast, $Dy_2Ti_2O_7$ exhibits the strongest relative field dependence, reaching about 25% at the lowest measured temperature. $DyYTi_2O_7$ shows a relative field dependence of around 17%. This strong field dependence in $Dy_2Ti_2O_7$ suggests that Dy^{3+} ions play a significant role in the suppression of κ_{xx}, consistent with previous findings [52,61,63]. Similar behavior and variation in the field dependence of κ_{xx} have been observed in the paramagnetic insulator $TmVO_4$ when the magnetic Tm^{3+} ion is replaced by Y^{3+} ions [62]. Furthermore, if we examine the field-dependent κ_{xx} of $DyYTi_2O_7$ at higher field values, above 15 K, it shows an increase in κ_{xx} compared to its zero-field value. In magnetically ordered materials, magnetic fluctuations around the ordering temperature can cause strong scattering of phonons, significantly suppressing the phononic heat conduction [63,64]. The application of a magnetic field partially suppresses these magnetic fluctuations, leading to the enhancement of phonon thermal conductivity [65]. $Dy_2Ti_2O_7$ and $DyYTi_2O_7$ do, however, not exhibit an increase in thermal conductivity with increasing field. Instead, their thermal conductivity decreases significantly at low temperatures and moderate fields, followed by a saturation at higher fields. With increasing temperature the overall field dependence rapidly decreases and finally results in a slight increase of κ_{xx} at higher fields and temperatures. This behavior can be related either to field-enhanced magnetic scattering on phonons [52,61,63] or to magnetoelastic coupling, and/or the presence of low-energy optical modes that intersect both longitudinal and transverse acoustic phonon modes [66]. These low-energy optical modes have been identified in various rare-earth pyrochlore materials, where their interference with acoustic phonon modes effectively reduces the overall lattice thermal conductivity [67]. In contrast, $Y_2Ti_2O_7$ shows a slight low-temperature increase in $\kappa_{xx}(B)$ of about 3%. At first glance, one might imagine this increase of $\kappa_{xx}(B)$ to be a consequence of possible magnetic impurities in $Y_2Ti_2O_7$. From the oxidation states $Y_2^{3+}Ti_2^{4+}O_7^{2-}$, magnetic impurities can arise when diamagnetic Ti^{4+} with $3d^0$ configuration, changes its oxidation state to Ti^{3+} with $3d^1$ and one Bohr magneton μ_B [68]. To investigate this possibility, we measured the magnetization of the single crystal used for the thermal transport measurements. However, on this small sample (6.3 mg), it was not possible to detect a reliable magnetization signal in our SQUID magnetometer. Thus, we measured the magnetization on a much larger piece (516 mg) from the same single crystal. As shown in Fig. 1, the magnetic susceptibility is almost constant and weakly diamagnetic ($\simeq -4 \times 10^{-5}$ emu/mol) above 100 K, then it slowly increases upon further cooling and reaches $\simeq 2 \times 10^{-4}$ emu/mol at 2 K. From a low-temperature magnetization curve up to 7 T (see Ref. [70]), we estimate the concentration of magnetic impurities to be below 0.05%. Therefore, we conclude that the slight low-temperature increase of κ_{xx} in $Y_2Ti_2O_7$ cannot be attributed to magnetic impurities and is likely of intrinsic origin. Furthermore, we conclude that the scattering of phonons by Dy^{3+} magnetic ions in $Dy_2Ti_2O_7$ and by both magnetic impurities and disorder in $DyYTi_2O_7$ is responsible for the significant suppression of κ_{xx} compared to nonmagnetic $Y_2Ti_2O_7$ in zero field.

We now shift our focus to the thermal Hall conductivity (κ_{xy}). Figures 2(a)–2(c) show linear magnetic field dependencies of κ_{xy} with negative signs for all samples and temperatures. From linear fits to the field-dependent $\kappa_{xy}(B)$ data measured at different temperatures, we derive the temperature-dependent κ_{xy}/B that is shown in Fig. 1(c). Note the negative sign of κ_{xy} for all three samples across the entire temperature range, which is in contrast to the positive κ_{xy} observed in $Tb_2Ti_2O_7$ [25,26]. For each sample, the temperature-dependent κ_{xy}/B shows a peak with a maximum value around the same temperature where a peak in κ_{xx} occurs. This coincidence of peaks in κ_{xx} and κ_{xy} has been reported in several insulating materials [18–21,26,27,32,34,35,40,42–45]. It is postulated that since κ_{xx}, being phonon-dominated, and given the concurrence of peak positions between κ_{xx} and κ_{xy}, κ_{xy} is also of phononic origin. To further check the phononic origin, we can examine the thermal Hall ratio (κ_{xy}/κ_{xx}), which represents the degree of handedness (chirality). It has been found that $|\kappa_{xy}|/\kappa_{xx}$ for numerous materials lies in the range of 10^{-4} to 10^{-3}, even though the absolute values of κ_{xx} and κ_{xy} vary by orders of magnitude at their peak temperatures [18–21,26,27,32,34,35,40,42–45]. The temperature dependence of κ_{xy}/κ_{xx} [see Fig. 3(a)] for all three samples decreases with increasing temperature, showing a maximum value within the same range of -10^{-4} to -10^{-3} for a magnetic field of 8 T. It is worth noting that the κ_{xy}/κ_{xx} measured for $Y_2Ti_2O_7$ is a sizable signal, contrary to what has been originally reported by Hirschberger *et al.* [25] and has been later cited as being zero by others [20,21,62]. The measured value of κ_{xy}/κ_{xx} suggests that the THE observed in all three samples is of phononic origin. This brings us to the central question: What is the underlying

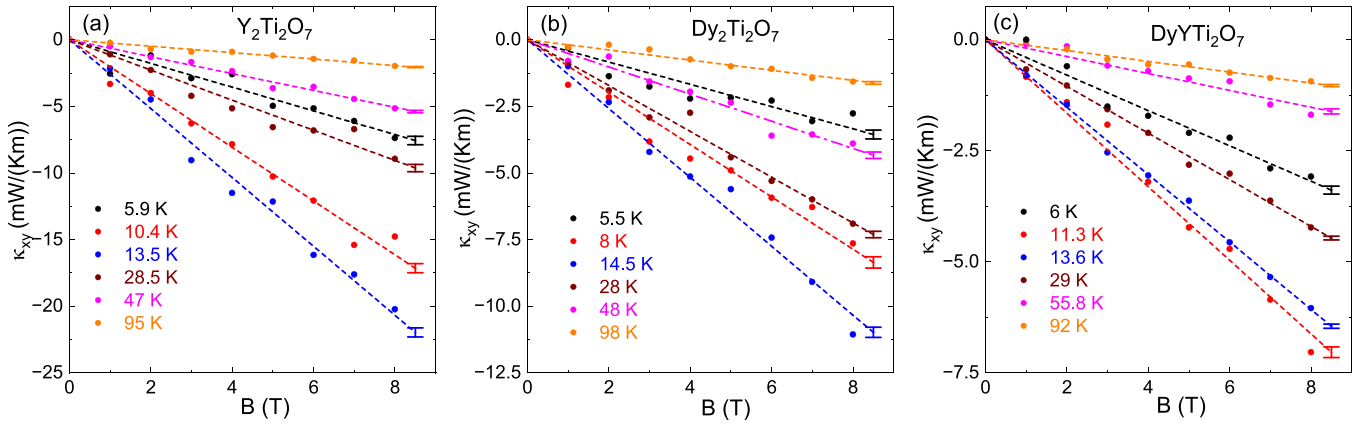

FIG. 2. (a)–(c) Field-antisymmetrized thermal Hall conductivities κ_{xy}(B) measured at constant temperatures on $Y_2Ti_2O_7$, $Dy_2Ti_2O_7$, and $DyYTi_2O_7$. The dashed lines are linear fits that were used to calculate the temperature-dependent κ_{xy}/B. For each fit, an error bar is calculated for $B = 8.5$ T using the standard deviation error of the obtained slope.

mechanism that causes phononic THE in these systems? For most of these materials, the microscopic origin of the THE has been attributed to phonons through two general coupling mechanisms. These mechanisms are either intrinsic, where phonons couple to a field-sensitive mechanism inherent to the host material, or extrinsic, where phonons couple through impurities and defects [69]. It is interesting to note that the value of κ_{xy}/κ_{xx} is nearly the same for all three samples at temperatures above 50 K. Below 50 K, the ratio κ_{xy}/κ_{xx} is largest in $Dy_2Ti_2O_7$ and smallest in $Y_2Ti_2O_7$, with the ratio in $DyYTi_2O_7$ only slightly exceeding that in $Y_2Ti_2O_7$. This rules out the possibility of a THE that is mainly arising from magnetic impurities. The enhanced κ_{xy}/κ_{xx} in $Dy_2Ti_2O_7$ below 50 K indicates that skew-scattering on magnetic Dy^{3+} ions has an additional impact, but this effect appears to be rather weak. Notably, a nonzero phononic THE has been observed in other nonmagnetic insulators [42,43,45], and it has been argued that the phonon THE is an intrinsic property of solids, which is supported by our observation of a phononic THE in nonmagnetic $Y_2Ti_2O_7$. Thus, we further explore the applicability of this intrinsic scenario across all three samples.

Recently, Li *et al.* [43] proposed a link between the universality of $|\kappa_{xy}|/\kappa_{xx}$ across different insulating materials and a characteristic length scale $\lambda_{\text{tha}} = \sqrt{\frac{\hbar}{eB}(\frac{\kappa_{xy}}{\kappa_{xx}})}$. This length scale λ_{tha} represents the correlation between the thermal Hall angle and the mean-free path for phonon Hall response. Interestingly, it was discovered that λ_{tha} varies only slightly, namely, from 2 Å to 7 Å, among these insulating materials, despite their phonon mean-free paths at the respective peak temperatures varying by up to four orders of magnitudes. Motivated by the study of Li *et al.* [43], we also generated similar plots and examined the range of λ_{tha} applicable to our samples.

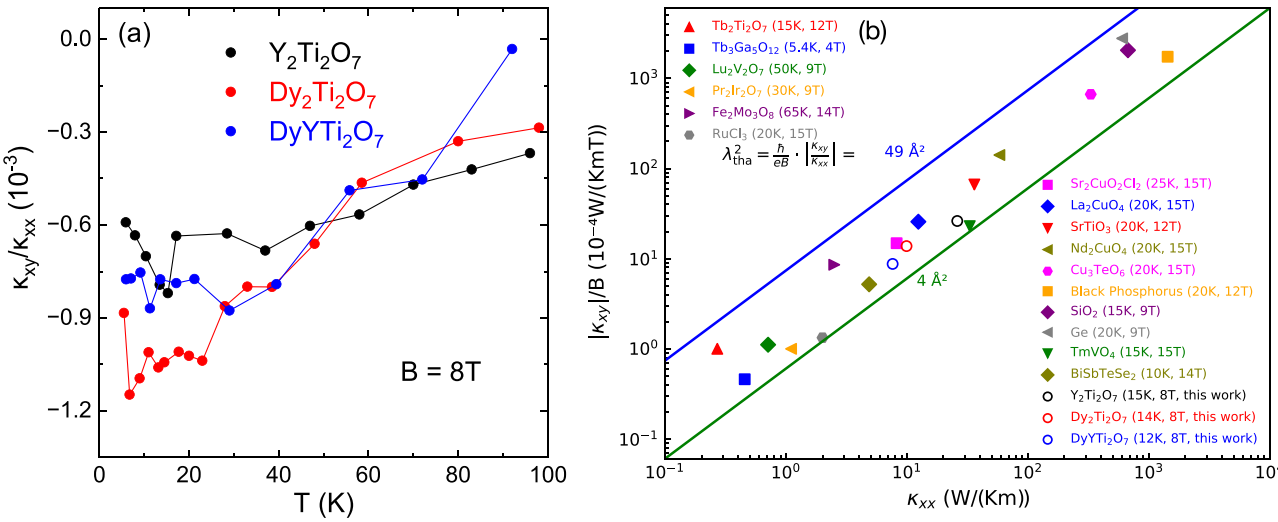

FIG. 3. (a) Temperature-dependent thermal Hall ratios κ_{xy}/κ_{xx} for $Y_2Ti_2O_7$, $Dy_2Ti_2O_7$, and $DyYTi_2O_7$. The maximum value of κ_{xy}/κ_{xx} remains in the range of -10^{-4} to -10^{-3}. (b) Scaling behavior of thermal Hall conductivities normalized by the field, $|\kappa_{xy}|/B$, and longitudinal thermal conductivities κ_{xx} of various insulators [17,19–21,23,24,26,34,42–45,62]. Using the magnetic length $\ell_B = \sqrt{\frac{\hbar}{eB}}$, the extracted length scale λ_{tha} from the relation $\lambda^2_{\text{tha}}/\ell^2_B = \kappa_{xy}/\kappa_{xx}$ remains between 2 Å to 7 Å for various insulators, despite their mean-free paths varying by orders of magnitude.

Intriguingly, the λ_{tha} values for all three samples are between 3 Å and 3.5 Å, falling within the range of 2 Å to 7 Å [see Fig. 3(b)]. It is noteworthy that due to the small variation of λ_{tha} among different solids, phonon THE has been proposed to be an intrinsic property of insulating solids, such as, e.g., $Y_2Ti_2O_7$. However, this scaling behavior holds true even in materials where extrinsic scenarios have been proposed [17,26,40,62]. This aligns with our observation of a weak impact on the thermal Hall ratio from the magnetic Dy^{3+} ions.

To conclude, we conducted a comparative study of thermal transport in $Y_2Ti_2O_7$, $Dy_2Ti_2O_7$, and $DyYTi_2O_7$ single crystals. The longitudinal thermal conductivities in all three samples are phonon-dominated. The presence of Dy^{3+} magnetic ions significantly affects κ_{xx}, as seen in the field-dependent data for $Dy_2Ti_2O_7$ and $DyYTi_2O_7$. We measured sizable field-linear thermal Hall conductivities κ_{xy} in all three samples. The temperature-dependent κ_{xy} show peaks around 15 K, coinciding with the respective peaks of κ_{xx}. The thermal Hall ratio, κ_{xy}/κ_{xx}, is large (approximately -10^{-4} to -10^{-3}) and aligns with other insulating materials where the THE of phononic origin has been reported [17, 19–21,23,24,26,34,42–45,62]. At low temperature, the thermal Hall ratio of $Dy_2Ti_2O_7$ is moderately enhanced in comparison to that of $Y_2Ti_2O_7$, suggesting that the phononic THE is of intrinsic origin for $Y_2Ti_2O_7$, but can be a combination of both intrinsic and extrinsic origin for $Dy_2Ti_2O_7$ and $DyYTi_2O_7$.

The data of this article are available from Zenodo [70].

We thank J. Frielingsdorf and M. Hiertz for the assistance in crystal growth and characterization and G. Grissonnanche for helpful discussions. We acknowledge support by the German Research Foundation via Project No. 277146847-CRC1238 (Subprojects A02 and B01).

[1] T. Qin, J. Zhou, and J. Shi, Berry curvature and the phonon Hall effect, Phys. Rev. B **86**, 104305 (2012).
[2] T. Saito, K. Misaki, H. Ishizuka, and N. Nagaosa, Berry phase of phonons and thermal Hall effect in nonmagnetic insulators, Phys. Rev. Lett. **123**, 255901 (2019).
[3] T. Ideue, Y. Onose, H. Katsura, Y. Shiomi, S. Ishiwata, N. Nagaosa, and Y. Tokura, Effect of lattice geometry on magnon Hall effect in ferromagnetic insulators, Phys. Rev. B **85**, 134411 (2012).
[4] L. Mangeolle, L. Balents, and L. Savary, Thermal conductivity and theory of inelastic scattering of phonons by collective fluctuations, Phys. Rev. B **106**, 245139 (2022).
[5] L. Mangeolle, L. Balents, and L. Savary, Phonon thermal Hall conductivity from scattering with collective fluctuations, Phys. Rev. X **12**, 041031 (2022).
[6] Y. Zhang, Y. Teng, R. Samajdar, S. Sachdev, and M. S. Scheurer, Phonon Hall viscosity from phonon-spinon interactions, Phys. Rev. B **104**, 035103 (2021).
[7] X. Zhang, Y. Zhang, S. Okamoto, and D. Xiao, Thermal Hall effect induced by magnon-phonon interactions, Phys. Rev. Lett. **123**, 167202 (2019).
[8] L. Sheng, D. N. Sheng, and C. S. Ting, Theory of the phonon Hall effect in paramagnetic dielectrics, Phys. Rev. Lett. **96**, 155901 (2006).
[9] R. Takahashi and N. Nagaosa, Berry curvature in magnon-phonon hybrid systems, Phys. Rev. Lett. **117**, 217205 (2016).
[10] H. Guo, D. G. Joshi, and S. Sachdev, Resonant thermal Hall effect of phonons coupled to dynamical defects, Proc. Natl. Acad. Sci. USA **119**, e2215141119 (2022).
[11] H. Guo and S. Sachdev, Extrinsic phonon thermal Hall transport from Hall viscosity, Phys. Rev. B **103**, 205115 (2021).
[12] H. Guo, Phonon thermal Hall effect in a non-Kramers paramagnet, Phys. Rev. Res. **5**, 033197 (2023).
[13] B. Flebus and A. H. MacDonald, Charged defects and phonon Hall effects in ionic crystals, Phys. Rev. B **105**, L220301 (2022).
[14] J.-Y. Chen, S. A. Kivelson, and X.-Q. Sun, Enhanced thermal Hall effect in nearly ferroelectric insulators, Phys. Rev. Lett. **124**, 167601 (2020).
[15] X.-Q. Sun, J.-Y. Chen, and S. A. Kivelson, Large extrinsic phonon thermal Hall effect from resonant scattering, Phys. Rev. B **106**, 144111 (2022).
[16] M. Mori, A. Spencer-Smith, O. P. Sushkov, and S. Maekawa, Origin of the phonon Hall effect in rare-earth garnets, Phys. Rev. Lett. **113**, 265901 (2014).
[17] C. Strohm, G. L. J. A. Rikken, and P. Wyder, Phenomenological evidence for the phonon Hall effect, Phys. Rev. Lett. **95**, 155901 (2005).
[18] G. Grissonnanche, A. Legros, S. Badoux, E. Lefrançois, V. Zatko, M. Lizaire, F. Laliberté, A. Gourgout, J. S. Zhou, S. Pyon, T. Takayama, H. Takagi, S. Ono, N. Doiron-Leyraud, and L. Taillefer, Giant thermal Hall conductivity in the pseudogap phase of cuprate superconductors, Nature (London) **571**, 376 (2019).
[19] G. Grissonnanche, S. Thériault, A. Gourgout, M. E. Boulanger, E. Lefrançois, A. Ataei, F. Laliberté, M. Dion, J. S. Zhou, S. Pyon, T. Takayama, H. Takagi, N. Doiron-Leyraud, and L. Taillefer, Chiral phonons in the pseudogap phase of cuprates, Nat. Phys. **16**, 1108 (2020).
[20] L. Chen, M.-E. Boulanger, Z.-C. Wang, F. Tafti, and L. Taillefer, Large phonon thermal Hall conductivity in the antiferromagnetic insulator Cu_3TeO_6, Proc. Natl. Acad. Sci. USA **119**, e2208016119 (2022).
[21] M.-E. Boulanger, G. Grissonnanche, S. Badoux, A. Allaire, É. Lefrançois, A. Legros, A. Gourgout, M. Dion, C. H. Wang, X. H. Chen, R. Liang, W. N. Hardy, D. A. Bonn, and L. Taillefer, Thermal Hall conductivity in the cuprate Mott insulators Nd_2CuO_4 and $Sr_2CuO_2Cl_2$, Nat. Commun. **11**, 5325 (2020).
[22] K. Sugii, M. Shimozawa, D. Watanabe, Y. Suzuki, M. Halim, M. Kimata, Y. Matsumoto, S. Nakatsuji, and M. Yamashita, Thermal Hall effect in a phonon-glass $Ba_3CuSb_2O_9$, Phys. Rev. Lett. **118**, 145902 (2017).
[23] T. Ideue, T. Kurumaji, S. Ishiwata, and Y. Tokura, Giant thermal Hall effect in multiferroics, Nat. Mater. **16**, 797 (2017).
[24] T. Uehara, T. Ohtsuki, M. Udagawa, S. Nakatsuji, and Y. Machida, Phonon thermal Hall effect in a metallic spin ice, Nat. Commun. **13**, 4604 (2022).

[25] M. Hirschberger, J. W. Krizan, R. J. Cava, and N. P. Ong, Large thermal Hall conductivity of neutral spin excitations in a frustrated quantum magnet, Science **348**, 106 (2015).

[26] Y. Hirokane, Y. Nii, Y. Tomioka, and Y. Onose, Phononic thermal Hall effect in diluted terbium oxides, Phys. Rev. B **99**, 134419 (2019).

[27] S. Sim, H. Yang, H.-L. Kim, M. J. Coak, M. Itoh, Y. Noda, and J.-G. Park, Sizable suppression of thermal Hall effect upon isotopic substitution in $SrTiO_3$, Phys. Rev. Lett. **126**, 015901 (2021).

[28] M. Hirschberger, R. Chisnell, Y. S. Lee, and N. P. Ong, Thermal Hall effect of spin excitations in a Kagome magnet, Phys. Rev. Lett. **115**, 106603 (2015).

[29] H.-L. Kim, T. Saito, H. Yang, H. Ishizuka, M. J. Coak, J. H. Lee, H. Sim, Y. S. Oh, N. Nagaosa, and J.-G. Park, Thermal Hall effects due to topological spin fluctuations in $YMnO_3$, Nat. Commun. **15**, 243 (2024).

[30] R. Hentrich, M. Roslova, A. Isaeva, T. Doert, W. Brenig, B. Büchner, and C. Hess, Large thermal Hall effect in α-$RuCl_3$: Evidence for heat transport by Kitaev-Heisenberg paramagnons, Phys. Rev. B **99**, 085136 (2019).

[31] H. Zhang, C. Xu, C. Carnahan, M. Sretenovic, N. Suri, D. Xiao, and X. Ke, Anomalous thermal Hall effect in an insulating van der Waals magnet, Phys. Rev. Lett. **127**, 247202 (2021).

[32] M.-E. Boulanger, G. Grissonnanche, É. Lefrançois, A. Gourgout, K.-J. Xu, Z.-X. Shen, R. L. Greene, and L. Taillefer, Thermal Hall conductivity of electron-doped cuprates, Phys. Rev. B **105**, 115101 (2022).

[33] C. Xu, C. Carnahan, H. Zhang, M. Sretenovic, P. Zhang, D. Xiao, and X. Ke, Thermal Hall effect in a van der Waals triangular magnet $FeCl_2$, Phys. Rev. B **107**, L060404 (2023).

[34] É. Lefrançois, G. Grissonnanche, J. Baglo, P. Lampen-Kelley, J. Q. Yan, C. Balz, D. Mandrus, S. E. Nagler, S. Kim, Y.-J. Kim, N. Doiron-Leyraud, and L. Taillefer, Evidence of a phonon Hall effect in the Kitaev spin liquid candidate α-$RuCl_3$, Phys. Rev. X **12**, 021025 (2022).

[35] S. Jiang, X. Li, B. Fauqué, and K. Behnia, Phonon drag thermal Hall effect in metallic strontium titanate, Proc. Natl. Acad. Sci. USA **119**, e2201975119 (2022).

[36] Q. Meng, X. Li, L. Zhao, C. Dong, Z. Zhu, and K. Behnia, Thermal Hall effect driven by phonon-magnon hybridization in a honeycomb antiferromagnet, arXiv:2403.13306 (2024).

[37] M. Gillig, X. Hong, C. Wellm, V. Kataev, W. Yao, Y. Li, B. Büchner, and C. Hess, Phononic-magnetic dichotomy of the thermal Hall effect in the Kitaev material $Na_2Co_2TeO_6$, Phys. Rev. Res. **5**, 043110 (2023).

[38] N. Li, R. R. Neumann, S. K. Guang, Q. Huang, J. Liu, K. Xia, X. Y. Yue, Y. Sun, Y. Y. Wang, Q. J. Li, Y. Jiang, J. Fang, Z. Jiang, X. Zhao, A. Mook, J. Henk, I. Mertig, H. D. Zhou, and X. F. Sun, Magnon-polaron driven thermal Hall effect in a Heisenberg-Kitaev antiferromagnet, Phys. Rev. B **108**, L140402 (2023).

[39] Y. Onose, T. Ideue, H. Katsura, Y. Shiomi, N. Nagaosa, and Y. Tokura, Observation of the magnon Hall effect, Science **329**, 297 (2010).

[40] A. Ataei, G. Grissonnanche, M.-E. Boulanger, L. Chen, É. Lefrançois, V. Brouet, and L. Taillefer, Phonon chirality from impurity scattering in the antiferromagnetic phase of Sr_2IrO_4, Nat. Phys. **20**, 585 (2024).

[41] M. Akazawa, M. Shimozawa, S. Kittaka, T. Sakakibara, R. Okuma, Z. Hiroi, H.-Y. Lee, N. Kawashima, J. H. Han, and M. Yamashita, Thermal Hall effects of spins and phonons in Kagome antiferromagnet Cd-kapellasite, Phys. Rev. X **10**, 041059 (2020).

[42] X. Li, B. Fauqué, Z. Zhu, and K. Behnia, Phonon thermal Hall effect in strontium titanate, Phys. Rev. Lett. **124**, 105901 (2020).

[43] X. Li, Y. Machida, A. Subedi, Z. Zhu, L. Li, and K. Behnia, The phonon thermal Hall angle in black phosphorus, Nat. Commun. **14**, 1027 (2023).

[44] R. Sharma, M. Bagchi, Y. Wang, Y. Ando, and T. Lorenz, Phonon thermal Hall effect in charge-compensated topological insulators, Phys. Rev. B **109**, 104304 (2024).

[45] X. Jin, X. Zhang, W. Wan, H. Wang, Y. Jiao, and S. Li, Discovery of universal phonon thermal Hall effect in crystals, arXiv:2404.02863 (2024).

[46] C. Castelnovo, R. Moessner, and S. L. Sondhi, Magnetic monopoles in spin ice, Nature (London) **451**, 42 (2008).

[47] D. J. P. Morris, D. A. Tennant, S. A. Grigera, B. Klemke, C. Castelnovo, R. Moessner, C. Czternasty, M. Meissner, K. C. Rule, J. U. Hoffmann, K. Kiefer, S. Gerischer, D. Slobinsky, and R. S. Perry, Dirac strings and magnetic monopoles in the spin ice $Dy_2Ti_2O_7$, Science **326**, 411 (2009).

[48] C. Paulsen, M. J. Jackson, E. Lhotel, B. Canals, D. Prabhakaran, K. Matsuhira, S. R. Giblin, and S. T. Bramwell, Far-from-equilibrium monopole dynamics in spin ice, Nat. Phys. **10**, 135 (2014).

[49] S. T. Bramwell and M. J. P. Gingras, Spin ice state in frustrated magnetic pyrochlore materials, Science **294**, 1495 (2001).

[50] D. Pomaranski, L. Yaraskavitch, S. Meng, K. Ross, H. Noad, H. Dabkowska, B. Gaulin, and J. Kycia, Absence of Pauling's residual entropy in thermally equilibrated $Dy_2Ti_2O_7$, Nat. Phys. **9**, 353 (2013).

[51] A. P. Ramirez, A. Hayashi, R. J. Cava, R. Siddharthan, and B. Shastry, Zero-point entropy in spin ice, Nature (London) **399**, 333 (1999).

[52] G. Kolland, M. Valldor, M. Hiertz, J. Frielingsdorf, and T. Lorenz, Anisotropic heat transport via monopoles in the spin-ice compound $Dy_2Ti_2O_7$, Phys. Rev. B **88**, 054406 (2013).

[53] G. Kolland, O. Breunig, M. Valldor, M. Hiertz, J. Frielingsdorf, and T. Lorenz, Thermal conductivity and specific heat of the spin-ice compound $Dy_2Ti_2O_7$: Experimental evidence for monopole heat transport, Phys. Rev. B **86**, 060402(R) (2012).

[54] S. Scharffe, G. Kolland, M. Valldor, V. Cho, J. Welter, and T. Lorenz, Heat transport of the spin-ice materials $Ho_2Ti_2O_7$ and $Dy_2Ti_2O_7$, J. Magn. Magn. Mater. **383**, 83 (2015).

[55] S. Scharffe, O. Breunig, V. Cho, P. Laschitzky, M. Valldor, J. F. Welter, and T. Lorenz, Suppression of Pauling's residual entropy in the dilute spin ice $(Dy_{1-x}Y_x)_2Ti_2O_7$, Phys. Rev. B **92**, 180405(R) (2015).

[56] H. Fukazawa, R. G. Melko, R. Higashinaka, Y. Maeno, and M. J. P. Gingras, Magnetic anisotropy of the spin-ice compound $Dy_2Ti_2O_7$, Phys. Rev. B **65**, 054410 (2002).

[57] W. H. Toews, J. A. Reid, R. B. Nadas, A. Rahemtulla, S. Kycia, T. J. S. Munsie, H. A. Dabkowska, B. D. Gaulin, and R. W. Hill, Disorder dependence of monopole dynamics in $Dy_2Ti_2O_7$ probed via thermal transport measurements, Phys. Rev. B **98**, 134446 (2018).

[58] R. Berman and R. Berman, *Thermal Conduction in Solids*, Oxford Studies in Physics (Clarendon Press, Oxford, UK, 1976).

[59] C. Kittel and P. McEuen, *Introduction to Solid State Physics* (John Wiley & Sons, New York, NY, 2018).

[60] Q. J. Li, Z. Y. Zhao, C. Fan, F. B. Zhang, H. D. Zhou, X. Zhao, and X. F. Sun, Phonon-glass-like behavior of magnetic origin in single-crystal $Tb_2Ti_2O_7$, Phys. Rev. B **87**, 214408 (2013).

[61] S. J. Li, Z. Y. Zhao, C. Fan, B. Tong, F. B. Zhang, J. Shi, J. C. Wu, X. G. Liu, H. D. Zhou, X. Zhao, and X. F. Sun, Low-temperature thermal conductivity of $Dy_2Ti_2O_7$ and $Yb_2Ti_2O_7$ single crystals, Phys. Rev. B **92**, 094408 (2015).

[62] A. Vallipuram, L. Chen, E. Campillo, M. Mezidi, G. Grissonnanche, M.-E. Boulanger, É. Lefrançois, M. P. Zic, Y. Li, I. R. Fisher, J. Baglo, and L. Taillefer, Role of magnetic ions in the thermal Hall effect of the paramagnetic insulator $TmVO_4$, Phys. Rev. B **110**, 045144 (2024).

[63] P. A. Sharma, J. S. Ahn, N. Hur, S. Park, S. B. Kim, S. Lee, J. G. Park, S. Guha, and S. W. Cheong, Thermal conductivity of geometrically frustrated, ferroelectric $YMnO_3$: Extraordinary spin-phonon interactions, Phys. Rev. Lett. **93**, 177202 (2004).

[64] K. Berggold, J. Baier, D. Meier, J. A. Mydosh, T. Lorenz, J. Hemberger, A. Balbashov, N. Aliouane, and D. N. Argyriou, Anomalous thermal expansion and strong damping of the thermal conductivity of $NdMnO_3$ and $TbMnO_3$ due to 4f crystal-field excitations, Phys. Rev. B **76**, 094418 (2007).

[65] Y. Tokiwa, T. Yamashita, M. Udagawa, S. Kittaka, T. Sakakibara, D. Terazawa, Y. Shimoyama, T. Terashima, Y. Yasui, T. Shibauchi, and Y. Matsuda, Possible observation of highly itinerant quantum magnetic monopoles in the frustrated pyrochlore $Yb_2Ti_2O_7$, Nat. Commun. **7**, 10807 (2016).

[66] M. Ruminy, M. N. Valdez, B. Wehinger, A. Bosak, D. T. Adroja, U. Stuhr, K. Iida, K. Kamazawa, E. Pomjakushina, D. Prabakharan, M. K. Haas, L. Bovo, D. Sheptyakov, A. Cervellino, R. J. Cava, M. Kenzelmann, N. A. Spaldin, and T. Fennell, First-principles calculation and experimental investigation of lattice dynamics in the rare-earth pyrochlores $R_2Ti_2O_7$ (R=Tb, Dy, Ho), Phys. Rev. B **93**, 214308 (2016).

[67] G. Lan, B. Ouyang, and J. Song, The role of low-lying optical phonons in lattice thermal conductance of rare-earth pyrochlores: A first-principle study, Acta Mater. **91**, 304 (2015).

[68] J. A. Rodriguez, A. Yaouanc, B. Barbara, E. Pomjakushina, P. Quémerais, and Z. Salman, Muon diffusion and electronic magnetism in $Y_2Ti_2O_7$, Phys. Rev. B **87**, 184427 (2013).

[69] V. Martelli, Phonons bend to magnetic fields, Nat. Phys. **20**, 537 (2024).

[70] R. Sharma, M. Valldor, and T. Lorenz, Dataset for the revised manuscript "Phonon thermal Hall effect in $Y_2Ti_2O_7$", Zenodo, doi:https://doi.org/10.5281/zenodo.13367786 (2024).